Journal of Modern Optics
Vol. 53, Nos. 16–17, 10–20 November 2006, 2519–2532

Taylor & Francis
Taylor & Francis Group

Coherent control of tunnelling dynamics in functionalized semiconductor nanostructures: a quantum-control scenario based on stochastic unitary pulses

L. G. C. REGO‡, S. G. ABUABARA† and V. S. BATISTA†*
†Department of Chemistry, Yale University, P.O. Box 208107, New Haven, CT, 06520-8107, USA
‡Department of Physics, Universidade Federal de Santa Catarina, Florianopolis, SC, 88040-900, Brazil

(*Received 15 February 2006; in final form 15 June 2006*)

The feasibility of achieving coherent control of tunnelling dynamics, associated with electronic excitations in functionalized semiconductor nanostructures, is investigated. The coherent control scenario is based on the application of frequent stochastic unitary pulses, affecting the interference phenomena between electronic wave-packet components and consequently the overall electronic tunnelling dynamics without collapsing the coherent quantum evolution of the system. It is shown that tunnelling can be inhibited and eventually halted by sufficiently frequent pulse fields that exchange energy with the system but do not affect the potential energy tunnelling barriers. Further, the proposed stochastic quantum-control scenario is demonstrated more generally as applied to an archetype model, a particle tunnelling in a quartic double-well potential.

1. Introduction

The development of coherent control techniques for optical manipulation of quantum tunnelling dynamics has become a subject of great research interest [1–9]. In particular, the study of dynamic localization and coherent destruction of quantum tunnelling [10–16] has attracted much attention due to the potential application of these effects in quantum computation [17–19]. Recent work [20] has explored the capabilities of deterministic sequences of 2π laser pulses as applied to the coherent manipulation of hole-tunnelling dynamics in functionalized semiconductor nanostructures [21]. This paper further investigates these techniques and extends them to coherent control based on randomized sequences of stochastic unitary pulses.

Functionalized semiconductor surfaces result from the adsorption of organic or inorganic molecules and the formation of surface complexes (see figure 1(*a*)).

*Corresponding author. Email: victor.batista@yale.edu

Journal of Modern Optics
ISSN 0950–0340 print/ISSN 1362–3044 online © 2006 Taylor & Francis
http://www.tandf.co.uk/journals
DOI: 10.1080/09500340600952036

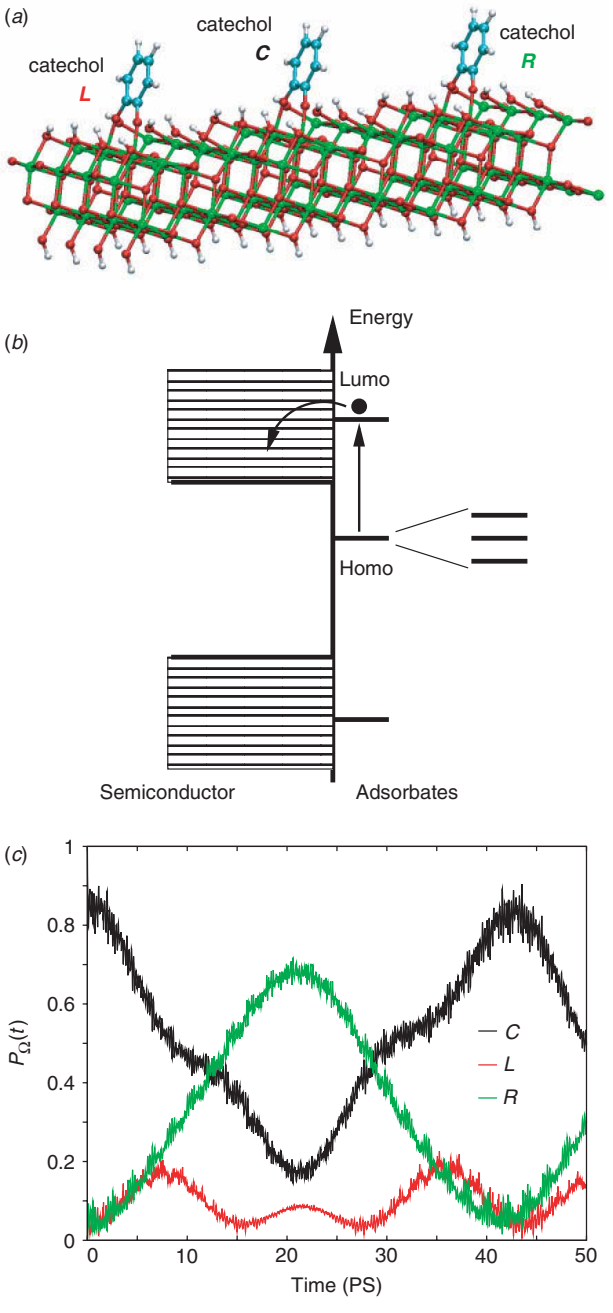

Figure 1. (*a*) TiO_2-anatase nanostructure functionalized with three catechol molecules; (*b*) energy diagram of the model system. The scheme shows the energy levels of the three surface-complexes (including splitting) and the photoinduced electron injection process depicted by the arrows. (*c*) Time-dependent electronic hole population transfer due to quantum tunnelling of superposition states, spatially localized on the three catechol adsorbates ($\mathbf{P}_j(t)$, $j \equiv L$ (left), C (centre), and R (right)), exhibiting spatial Rabi oscillations. (The colour version of this figure is included in the online version of the journal.)

As a result, interband electronic states are introduced in the semiconductor band gap, sensitizing the host material for photoabsorption at frequencies characteristic of the molecular adsorbates (see energy level diagram in figure 1(*b*)). Photoexcitation of surface complexes often leads to electron–hole pair separation, due to ultrafast interfacial electron injection, when there is suitable energy match between the photoexcited molecular state localized in the surface complex and the electronic states in the conduction band of the semiconductor material [21–25], a process that leaves electron–holes in the manifold of interband states, i.e. off-resonance relative to the semiconductor valence and conduction bands. Along with the hole wavepacket's localization on the adsorbate, this off-resonance condition decouples the electron–holes from certain dephasing mechanisms, extending their lifetime beyond that normally observed for excitations in room-temperature semiconductors.

Recent theoretical work has addressed the time-scales and mechanisms of interfacial electron transfer in TiO_2-anatase functionalized with catechol molecules [22], a simple prototype of aromatic anchoring ligand, upon which more complex molecular structures can be attached for specific applications [26]. Further studies have focused on the subsequent relaxation dynamics of hole states [21], after electron–hole pair separation, as well as on the feasibility of coherent optical manipulation of the dynamics of hole states by the application of deterministic sequences of femtosecond 2π pulses [20]. Building upon these earlier studies [20–22], this paper addresses the nontrivial question as to whether the underlying super-exchange hole-tunnelling dynamics can also be coherently controlled by the application of stochastic sequences of unitary pulses, without collapsing the coherent quantum evolution of the system.

The reported computational results show that the frequent application of stochastic unitary pulses affects the overall tunnelling dynamics by altering the interference phenomena between electronic wave-packet components, inducing coherent energy exchange between the system and the perturbational field. The underlying coherent control mechanism is therefore significantly different from other dynamical localization schemes where the coherent destruction of quantum tunnelling is achieved by the application of an external driving field that collapses the coherent quantum evolution of the system [27], or modulates the potential energy tunnelling barrier with periodic [11, 12], or stochastic [28] perturbations. For completeness, the proposed stochastic quantum control scenario is demonstrated in a more general model system exhibiting common quantum relaxation dynamics, tunnelling in a double-well potential.

2. Structural models

We consider a model system composed of catechol molecules adsorbed on the (101) surface of the TiO_2-anatase semiconductor, as depicted in figure 1(*a*). The dimensions of the nanostructure are $3 \times 1.5 \times 3$ nm along the [−101], [010] and [101] directions, respectively, with adjacent adsorbates 1 nm apart. The surface dangling bonds are saturated with hydrogen capping atoms in order to quench the formation of surface states [29], avoiding nonphysical low

coordination numbers. Periodic boundary conditions are imposed with a vacuum spacer between slabs, making negligible the interaction between distinct surfaces in the infinitely periodic model system. Geometry relaxation as well as thermalization and equilibration under conditions of room temperature and constant volume are performed using the Vienna *ab initio* Simulation Package (VASP/VAMP) [30–32]. The resulting structural relaxation next to the adsorbate describes the underlying surface reconstruction due to functionalization [22, 33], a process that is partially responsible for quenching the formation of surface states deep within the semiconductor band gap [29].

3. Quantum dynamics simulations

The superexchange hole-tunnelling dynamics, after electron–hole pair separation, is described according to an approximate mixed quantum–classical method in which the electrons are treated quantum mechanically and the nuclei classically. The nuclei evolve on an effective mean-field Potential Energy Surface (PES), according to classical trajectories $\mathbf{R}^{\xi} = \mathbf{R}^{\xi}(t)$ with initial conditions specified by index ξ. Results are obtained by sampling an ensemble of initial conditions ξ for nuclear motion, integrating the time-dependent Schrödinger equation (TDSE), over the corresponding *ab initio*-DFT nuclear trajectories and averaging expectation values over the resulting time-evolved wavefunctions. Converged results for finite temperature simulations are typically obtained by averaging over fewer than 50 initial conditions, representing the system thermalized under conditions of room temperature and constant volume. However, finite temperature results are reported for averages over 100 initial conditions. The appreciation of conditions under which quantum coherences may be described according to mixed quantum–classical methodologies has been the subject of intense research [34–37], including the analysis of decoherence in similar composite models [38, 39]. The applicability of mixed quantum–classical dynamics is found to be valid so long as the quantum subsystem (electronic dynamics) decoheres slowly and the remainder (nuclear dynamics), often coupled to a thermal bath, decoheres quickly [40].

Propagation of the time-dependent electronic wavefunction is performed for each nuclear trajectory $\mathbf{R}^{\xi}(t)$ by numerically exact integration of the TDSE, $\{i\hbar\partial/\partial t - \mathbf{H}(t)\}|\Psi^{\xi}(t)\rangle = 0$. Here, $\mathbf{H}(t)$ is described according to a tight binding model Hamiltonian gained from the extended Hückel (EH) approach [41, 42]. The EH Hamiltonian is computed in the basis of Slater-type orbitals χ for the radial part of the atomic orbital (AO) wavefunctions [22, 43], including the 4s, 4p and 3d atomic orbitals of Ti^{4+} ions, the 2s and 2p atomic orbitals of O^{2-} ions, the 2s and 2p atomic orbitals of C atoms, and the 1s atomic orbitals of H atoms. The AOs $\{|\chi_{\alpha}(t)\rangle\}$ form a mobile (nonorthogonal) basis set due to nuclear motion, with $S_{\alpha\beta}(t) = \langle\chi_{\alpha}(t)|\chi_{\beta}(t)\rangle$ the corresponding time-dependent overlap matrix elements. The overlap matrix is computed using periodic boundary conditions along the [010] or [−101] directions, for the [−101] and [010] extended systems, respectively. Advantages of this method, relative to plane-wave approaches, are that it

requires a relatively small number of transferable parameters and is capable of providing accurate results for the energy bands of elemental materials (including transition metals) as well as compound bulk materials in various phases [42]. In addition, the EH method is applicable to large extended systems and provides valuable insight on the role of chemical bonding [44].

The time-dependent hole wavefunction, $|\Psi^{\xi}(t)\rangle = \sum_q B_q(t)|\phi_q(t)\rangle$, is expanded in the basis of instantaneous eigenstates $|\phi_q(t)\rangle = \sum_\alpha C_{\alpha,q}(t)|\chi_\alpha(t)\rangle$ of the generalized eigenvalue problem $\mathbf{H}(t)\mathbf{C}(t) = \mathbf{S}(t)\mathbf{C}(t)\mathbf{E}(t)$, with eigenvalues $E_q(t)$. It is assumed that the initial state, after electron–hole pair separation, consists of a hole localized in the highest occupied molecular orbital (HOMO) of the central (C) surface complex. The propagation scheme is based on the recursive application of the short-time approximation $|\Psi^{\xi}(t+\tau/2)\rangle \approx \sum_q B_q(t)e^{-(i/\hbar)E_q(t)\tau/2}|\phi_q(t)\rangle$. The evolution of the expansion coefficients $B_q(t+\tau) = \sum_p B_p(t)e^{-(i/\hbar)\left[E_p(t)+E_q(t+\tau)\right]\tau/2}\langle\phi_q(t+\tau)|\phi_p(t)\rangle$ is approximated by $B_q(t+\tau) \approx B_q(t)e^{-(i/\hbar)\left[E_q(t)+E_q(t+\tau)\right]\tau/2}$, in the limit of sufficiently thin time-slices τ.

The relaxation dynamics is quantitatively described in terms of expectation values of observables computed as $\langle\hat{A}\rangle = \mathsf{Tr}\{\hat{\rho}(t)\hat{A}\}$, where $\hat{\rho}(t)$ is the reduced density operator associated with the electronic degrees of freedom, $\hat{\rho}(t) = \sum_\xi p_\xi|\Psi^{\xi}(t)\rangle\langle\Psi^{\xi}(t)|$, with p_ξ the probability of sampling initial conditions, specified by index ξ, associated with the thermal ensemble of nuclear configurations.

The time-dependent hole populations are determined as follows: $\mathbf{P}_j(t) = \mathsf{Tr}\{\hat{\rho}(t)\hat{P}_j\}$, where $\hat{P}_j$ is the projection operator onto the subset of atomic orbitals of interest. Computations of the transient hole populations $\mathbf{P}_j(t)$ of the molecular adsorbates $j = (L, C, R)$ are defined accordingly, $\hat{P}_j = \sum_{\alpha,\,\beta\in j}|\chi_\alpha\rangle\left(S^{-1}\right)_{\alpha\beta}\langle\chi_\beta|$, where the sum over atomic orbitals includes atoms of adsorbate j only.

The resulting relaxation dynamics is essentially described by spatial Rabi-like oscillations (see figure 1(*c*)), i.e. coherent electronic population transfer between adjacent adsorbates, despite the partial intrinsic decoherence induced by thermal ionic motion [20, 21]. The underlying superexchange hole-tunnelling between adsorbate molecules results from scattering events where near-resonant states localized on adsorbate molecules become indirectly coupled by mediating states in the semiconductor host substrate. These events last approximately 100 fs and occur once or twice every picosecond as thermal fluctuations modulate the electronic couplings and resonance conditions. Therefore, the model predicts observable Rabi oscillations if mediating states in the semiconductor have lifetimes longer than the duration of a single scattering event (e.g. 1 ps) [20]. The coherent population transfer among adjacent adsorbates is mainly stabilized by the finite size of the nanostructure, where the adsorbate states, while coupled by the common host substrate, remain off-resonant relative to the valence and conduction bands (manifolds) of electronic states. carrier–phonon, and likely carrier–carrier, scattering mechanisms which would otherwise lead to the commonly observed ultrafast decoherence in semiconductor spectroscopy are highly suppressed by the off-resonance and symmetry conditions of the electronic states in surface complexes. Further, under vacuum conditions, geminate recombination of injected electrons (back-transfer) is much slower, occuring in the nanosecond regime [45].

4. Coherent control

The coherent control scenario implemented in this paper constitutes a generalization of the recently reported quantum control scheme based on deterministic 2π unitary pulses [20]. These coherent control scenarios are inspired in other similar approaches for modulating quantum relaxation dynamics, also based on sequences of unitary pulses [46–49]. All such approaches preserve the coherent nature of unitary evolution and therefore are particularly suited to quantum information processing applications.

In the present generalization to stochastic coherent control, the time evolution operator for an optical pulse coupling the initially populated state $|1\rangle$ with and auxiliary state $|2\rangle$ is

$$\hat{U}^{\Phi} = \cos\left[\frac{\Gamma \cdot \tau}{2}\right](|1\rangle\langle 1| + |2\rangle\langle 2|) - i\sin\left[\frac{\Gamma \cdot \tau}{2}\right](|1\rangle\langle 2| + |2\rangle\langle 1|), \tag{1}$$

where $\Phi = \Gamma \cdot \tau/2$ is a random phase, defined by the product of the optical Rabi frequency Γ and a random effective pulse duration τ (duration of the resonance between Γ and the desired optical transition). In the particular case of $\Gamma \cdot \tau = 2\pi$, the time evolution operator becomes the deterministic 2π pulse, $\hat{U}^{2\pi}_{2\times 2} = -|1\rangle\langle 1| - |2\rangle\langle 2|$, inducing only a π phase-shift $|\Psi_{2\pi}\rangle = \hat{U}^{2\pi}|\Psi\rangle$ in the time-evolved wave-packet component corresponding to state $|1\rangle$ so long as $\langle 2\,|\,\Psi\rangle = 0$. In the present application to coherent control of superexchange hole-tunnelling dynamics in functional semiconductors, $|1\rangle$ denotes the HOMO of the central catechol, $|\phi_C\rangle$, and $|2\rangle$ is an auxiliary state of the same adsorbate (e.g., the catechol-(HOMO-1), similarly off-resonant to the semiconductor valence and conduction bands). Note, that if the pulsed light does not interact with any of the other $N-2$ states within an N-level system, the full time evolution operator is thus the sum $\mathbf{I}_{(N-2)\times(N-2)} + \hat{U}^{2\pi}_{2\times 2} = \mathbf{I}_{N\times N} - \mathbf{I}_{2\times 2} + \hat{U}^{2\pi}_{2\times 2}$. Furthermore, since $\Psi_0 \equiv |\Psi(t=0)\rangle \approx |\phi_C\rangle$, the 2π pulse time evolution operator can be numerically implemented as the unitary operator, $\hat{U}^{2\pi} = \mathbf{I} - 2|\Psi_0\rangle\langle\Psi_0|/\langle\Psi_0|\Psi_0\rangle = \mathbf{I} - 2|\Psi_0\rangle\langle\Psi_0|$, as reported in previous work [20], where $\mathbf{I}$ is the identity matrix and $\langle\Psi_0|\Psi_0\rangle = 1$.

4.1 *Inhibiting tunnelling in functionalized semiconductors*

Figure 2, panel (a), shows the time-dependent hole populations $\mathbf{P}_j$ of adsorbates $j = (C, R, L)$, exhibiting Rabi oscillations due to superexchange hole tunnelling dynamics in the absence of perturbational pulses. In contrast, panels (b) and (c) compare the perturbational effects of sequences of 2π pulses (panel b) and stochastic phase-kick pulse on the underlying hole relaxation dynamics. Both sequences of pulses are applied in the 16–40 ps time window (indicated with arrows). The 2π pulses are applied at intervals of 200 fs, while the random-phase kicks are applied at stochastic intervals with average spacing of 200 fs. It is shown that the main effect of sequences of (deterministic or stochastic) unitary pulses is to suspend Rabi oscillations, keeping approximately constant the hole population of the adsorbate R. These results demonstrate that coherent control scenarios based on frequent unitary pulses are robust with respect to stochasticity, efficiently inhibiting

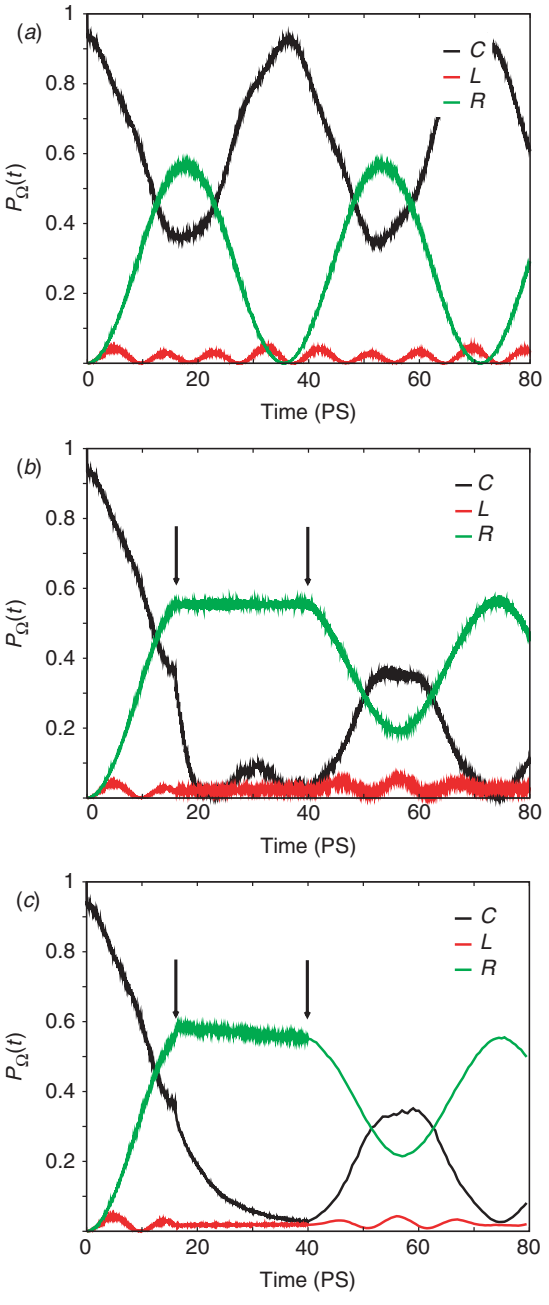

Figure 2. Time-dependent hole populations P_j of adsorbates $j = (C, R, L)$ for the cases (*a*) no pulses; (*b*) instantaneous 2π pulses implemented at regular 200 fs intervals; (*c*) random-phase pulses implemented at stochastic intervals with average 200 fs. (The colour version of this figure is included in the online version of the journal.)

superexchange tunnelling dynamics among adjacent catechol adsorbed on functionalized TiO_2-substrates under low temperature and vacuum conditions.

4.2 *Steering tunnelling in functionalized semiconductors*

This section considers the implementation of sequences of unitary pulses for steering, rather than inhibiting, the underlying hole-tunnelling dynamics in the functionalized semiconductors. It is shown that phase-kick pulses can affect the tunnelling period and even directionality, when timed to coincide with certain points along the relaxation dynamics. For example, a π phase kick sequence timed to begin and applied at intervals corresponding with the maximum amplitude of population transfer between two adsorbates can reset the dynamics and reverse the incipient direction of tunnelling. This behaviour is illustrated in figure 3(*a*), where a well-timed pulse sequence can double the oscillation period between the centre and right adsorbates (compare to figure 2(*a*)). Timing phase kick intervals to correspond with half-period intervals applied at inflection points in the coherent population transfer dynamics, on the other hand, result in reversal of convexity in the dynamics and an effective directionality reversal. This contrary behaviour is illustrated in figure 3(*b*), where hole population is driven towards the left adsorbate, again merely by implementing 2π pulses coupling the centre adsorbate to an auxiliary state, resulting in a π phase kick of a component of the time-evolved wavepacket.

Intuition guiding these tantalizing results may be arrived at with a simple analysis: adopting a truncation approximation to the time-dependent wavefunction of the hole, $|\Psi(t)\rangle \equiv |\Psi\rangle = B_C e^{-i\omega_C t}|\phi_C\rangle + B_R e^{-i\omega_R t}|\phi_R\rangle + B_L e^{-i\omega_L t}|\phi_L\rangle + |\varepsilon\rangle$, where $B_j = B_j(0)$ and $|\varepsilon\rangle$ is the error made in the truncation. A typical nuclear configuration yields the following spectral distribution for the wavepacket: $|B_C|^2 + |B_R|^2 + |B_L|^2 = 0.779 + 0.175 + 0.012 \approx 97\%$, thus $\langle\varepsilon|\varepsilon\rangle \approx 0.03 \ll 1$. Notice that the MOs $|\phi_C\rangle$, $|\phi_R\rangle$, $|\phi_L\rangle$, and the vector $|\varepsilon\rangle$ are orthogonal to each other. Thus, at $t = 0$

$$|\Psi(0)\rangle \equiv |\Psi_0\rangle \approx B_C|\phi_C\rangle + B_R|\phi_R\rangle + B_L|\phi_L\rangle, \tag{2}$$

and after the incidence of a 2π pulse, the transformed wavefunction $|\Psi_{2\pi}\rangle = \hat{U}_{2\pi}|\Psi\rangle$ is

$$\begin{aligned}|\Psi_{2\pi}\rangle &\approx \left[1 - 2\xi(t)e^{i\omega_C t}\right]B_C(t)|\phi_C\rangle + \left[1 - 2\xi(t)e^{i\omega_R t}\right]B_R(t)|\phi_R\rangle + \left[1 - 2\xi(t)e^{i\omega_L t}\right]B_L(t)|\phi_L\rangle \\ &\approx \Omega_C(t)B_C(t)|\phi_C\rangle + \Omega_R(t)B_R(t)|\phi_R\rangle + \Omega_L(t)B_L(t)|\phi_L\rangle, \end{aligned} \tag{3}$$

where $\xi(t) = \langle\Psi_0|\Psi\rangle$ is the time-dependent autocorrelation function and $\omega_j = E_j/\hbar$. If nuclear dynamics is included we have $E_j = E_j(t)$ and $\omega_j(t)$.

The moduli of the coefficients $|B_j(t)|^2 = |B_j(0)|^2$ are merely constant values that determine the spectral distribution of the wave-packet. Therefore, equation (3) indicates that 2π pulses can be used to control the localization of the wave-packet among the adsorbates, due to the time dependence of the $\Omega_j(t)$ $(j = L, C, R)$. The $|\Omega_j(t)|$ are presented in figure 3(*c*) for the fully relaxed atomic configuration used in this work. The oscillatory behaviour is easily understood: one obtains for the $\Omega_C(t)$ term

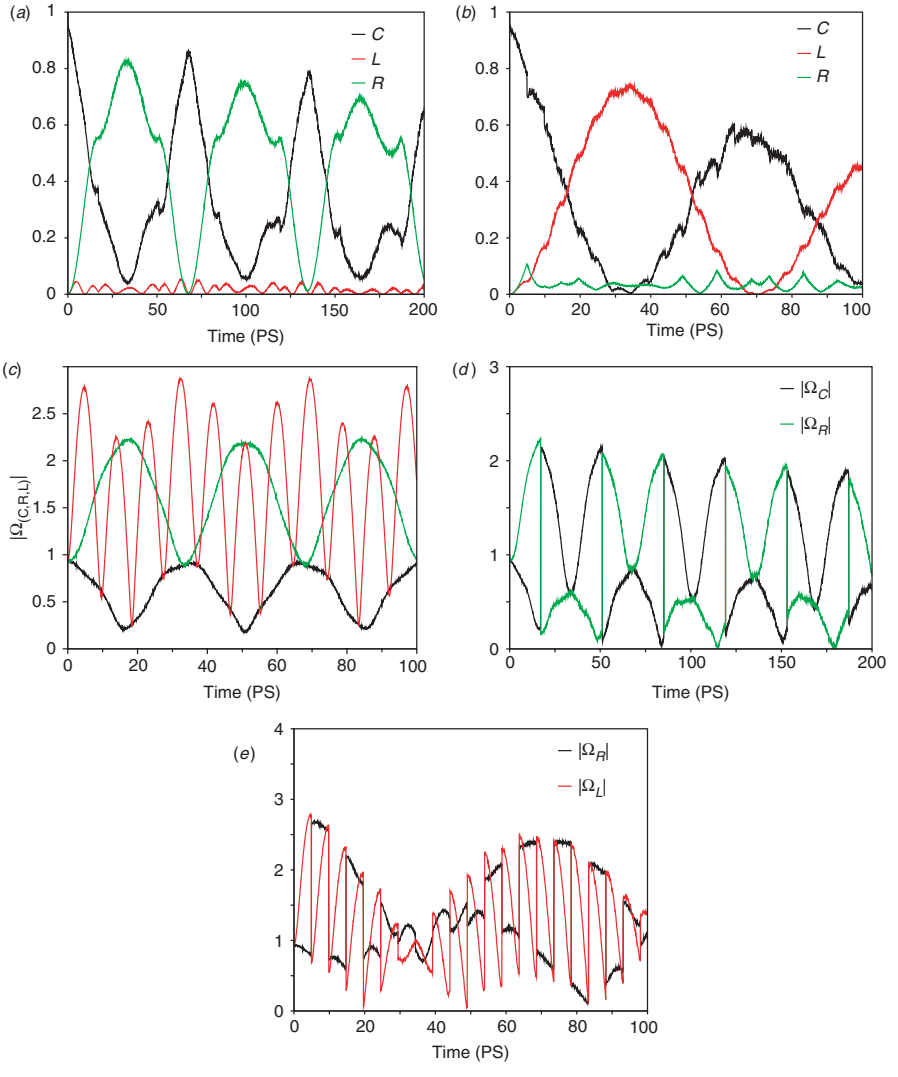

Figure 3. (*a*) Hole populations $P_j(t)$ in the adsorbate–semiconductor system produced by a train of pulses at intervals $\tau = T_{CR}$. (*b*) Hole populations produced by a train of pulses at intervals $\tau = T_{LC}/2$. (*c*) $|\Omega_j(t)|$ as a function of time for $j = C$ (black), R (green) and L (red), for the fully relaxed nanostructure (low temperature nuclear configuration). (*d*) $|\Omega_{(C,R)}(t)|$ for pulses implemented at intervals $\tau = T_{CR}$. (*e*) corresponding $|\Omega_{(C,L)}(t)|$ for pulses at intervals $\tau = T_{LC}/2$. (The colour version of this figure is included in the online version of the journal.)

$$\Omega_C(t) = \left[1 - 2\xi(t)e^{i\omega_C t}\right] \tag{4}$$

$$= \left[1 - 2|B_C|^2 - 2\left(|B_R|^2 e^{i\omega_{CR}t} + |B_L|^2 e^{i\omega_{CL}t}\right)\right], \tag{5}$$

with $\omega_{CR} = \omega_C - \omega_R$ and $\omega_{CL} = \omega_C - \omega_L$.

For the scenario we are investigating, i.e. initial photo-excitation of the central catechol, a general nuclear configuration produces $|B_C|^2 \gg |B_R|^2 \gg |B_L|^2$. Thus the

major harmonic contribution to $\Omega_C(t)$ comes from ω_{CR}. The maxima of $\Omega_C(t)$, therefore, must occur when $\omega_{CR}\tau = 2\pi$, more generally at $\tau = nT_{CR}$ where T_{CR} is the tunnelling period between the centre and right adsorbate, yielding

$$\Omega_C(\tau) = \left[1 - 2(|B_C|^2 + |B_R|^2) - 2|B_L|^2 e^{i\omega_{CL}\tau}\right] \tag{6}$$
$$\approx [1 - 2] \longrightarrow |\Omega_C(t)| \approx 1.$$

The minima occur at $\tau = (n + 1/2)T_{CR}$,

$$\Omega_C(\tau) = \left[1 - 2|B_C|^2 + 2|B_R|^2 - 2|B_L|^2 e^{i\omega_{CL}\tau}\right] \tag{7}$$
$$\approx \left[1 - 2|B_C|^2 + 2|B_R|^2\right]. \tag{8}$$

In general $|B_C|^2 > 0.5$, implying $|\Omega_C(\tau)| < 0.5$ at $\tau = (n + 1/2)T_{CR}$.

Accordingly for $\Omega_R(t)$,

$$\Omega_R(t) = \left[1 - 2|B_R|^2 - 2\left(|B_C|^2 e^{i\omega_{RC}t} + |B_L|^2 e^{i\omega_{RL}t}\right)\right]. \tag{9}$$

Here, also, ω_{RC} is the more important spatial Rabi frequency. However, the minima occur at $\tau = nT_{CR}$, whereas the maxima at $\tau = (n + 1/2)T_{CR}$ (refer to figure 3(*c*)). Finally, the coefficient $\Omega_L(t)$ is

$$\Omega_L(t) = \left[1 - 2|B_L|^2 - 2\left(|B_C|^2 e^{i\omega_{LC}t} + |B_R|^2 e^{i\omega_{LR}t}\right)\right] \tag{10}$$
$$\approx \left[1 - 2\left(|B_C|^2 e^{i\omega_{LC}t} + |B_R|^2 e^{i\omega_{LR}t}\right)\right]. \tag{11}$$

In this case, the most important spatial Rabi frequency is ω_{LC} and $T_{LC} = 2\pi/\omega_{LC} \approx 9.6$ ps. Therefore, the maxima of $|\Omega_L(t)|$ occur at $\tau = (n + 1/2)T_{LC}$, yielding $|\Omega_L| \approx 1 + 2|B_C|^2$, if $|B_C|^2 \gg |B_R|^2$. The minima occur at $\tau = nT_{LC}$ yielding $|\Omega_L| \approx |1 - 2|B_C|^2|$.

Thus, figure 3(*c*) shows that applying a second 2π pulse at $\tau \approx 17$ ps, once the spectral distribution of the wave-packet has changed coherently from molecule C toward molecule R as the weights corresponding to B_C and B_R are approximately exchanged, should markedly affect the tunnelling dynamics. Therefore, subsequent applications of 2π pulses at intervals T_{CR} could drive the hole through an effective spatial Rabi oscillation of period $T = 2T_{CR}$, as was shown in figure 3(*a*), with the corresponding behaviour of $|\Omega_{(C,R)}(t)|$ for this sequence of pulses shown in figure 3(*d*). Conversely, applying 2π pulses at intervals $\tau = T_{CL}/2$ causes the spectral distribution of the wavepacket to move gradually towards molecule L, as was demonstrated by figure 3(*b*). The maximum hole population at molecule L, then, reaches 0.7, which is much higher than the values obtained under regular dynamics for that adsorbate. Figure 3(*e*) exhibits the dynamics of $|\Omega_{(C,L)}(t)|$ for the necessary sequence of pulses.

4.3 *Coherent control of tunnelling in a quartic double-well*

This section demonstrates the quantum control scenario, based on frequent stochastic unitary pulses, as applied to an archetype model: a particle tunnelling in the quartic double-well potential described by the Hamiltonian, $\hat{H} = (\hat{p}^2/2m) - \alpha\left(\hat{x}^2 - \beta\hat{x}^4\right)$.

Figure 4 shows the time-dependent probability of finding the particle on either side of the tunnelling barrier during the first 80 ps of dynamics. A comparison of the underlying tunnelling dynamics, in the absence of perturbational pulses (panel a), or perturbed by deterministic (panel b) or stochastic (panel c) unitary pulses in the time window 35–50 ps, is presented. Here, each pulse adds a phase shift to the component of the time-dependent wavefunction corresponding the initial state. For the case of π phase kicks, the phase manipulation could plausibly be effected by a sequence of ultrashort 2π pulses coupling each of the two lowest energy levels of the double well potential surface respectively to two distinct levels of an auxiliary surface (one symmetric, one antisymmetric to obey parity selection rules resulting from considering the dipole operator). The simulation results for this case, presented in figure 4(*b*), clearly demonstrate that a regular sequence of π phase kicks applied to a component of the time-evolved wave-packet can inhibit tunnelling dynamics yet preserve coherence, since the coherent tunnelling dynamics continues after termination of the pulse sequence. Figure 4(*c*) presents two generalizations of this scheme, in which the intervals between kicks, and both the intervals and the phase kicks themselves, are randomized.

The demonstrated inhibition of tunnelling accomplishes the same effect of the phenomenon termed coherent destruction of tunnelling [16], first reported by Grossman and co-workers. [11]. In those driven tunnelling models, a (usually monochromatic) oscillatory term in the Hamiltonian modulates the potential barrier and may inhibit tunnelling or localize the wave-packet. [50] The relationship between the present scheme, in which only the phase of only a component of the wavefunction is affected in an interaction instantaneous compared to the timescales determined by the potential barrier, but with some comparable periodicity, i.e. the pulses come at intervals relevant to the natural timescales of the dynamical system, will be presented elsewhere [51].

5. Conclusions

The investigation of an atomistic model of functionalized TiO_2-anatase suggests that stochastic sequences of unitary pulses could be used to coherently control electronic excitations in semiconductor surface complexes. The already widespread study of such inexpensive, versatile, and tunable systems should make them valuable avenues for the investigation of fundamental quantum dynamics, complementing other well-studied mesoscopic systems such as doped semiconductor materials and quantum dots.

We have shown that stochastic optical pulses and functionalized semiconductors could be used to feasibly implement a bang–bang coherent control scheme in this readily available and relatively pedestrian environment. The observed coherent tunnelling dynamics can be dramatically affected by phase kicks altering the underlying relaxation dynamics without collapsing the unitary evolution of the system. Furthermore, it is shown that sequences of unitary pulses can also be designed to coherently steer quantum tunnelling dynamics of electronic populations in functionalized semiconductor materials. It is therefore conjectured that the ability

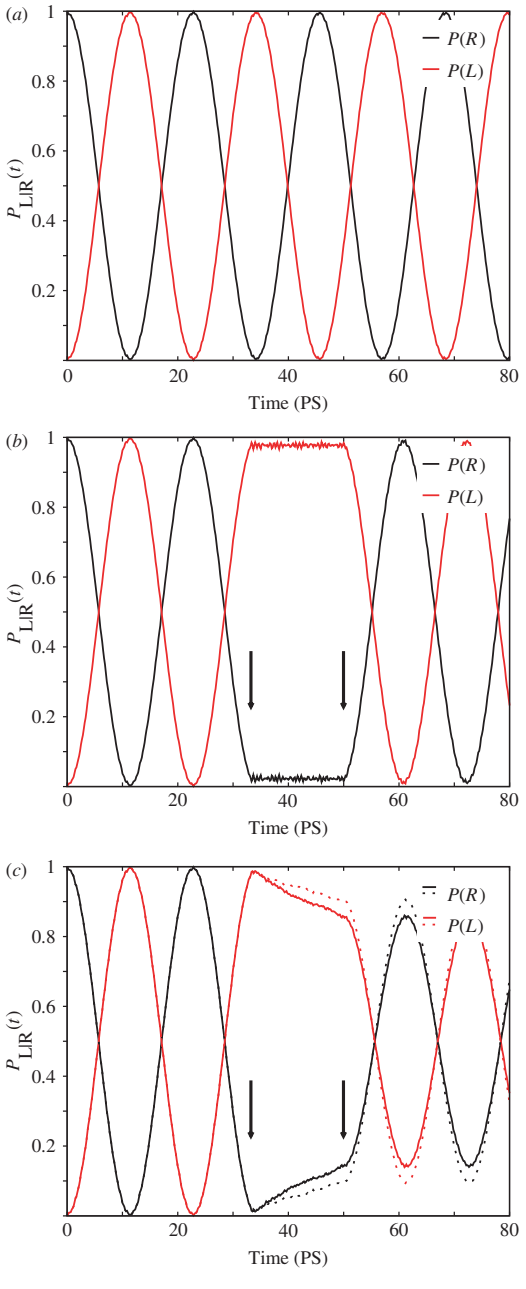

Figure 4. Probability of a particle being found in the right (black) or left (red) well for quantum tunnelling dynamics in a quartic double oscillator. The figure depicts evolution in the cases of (*a*) no kicks; (*b*) π phase kicks at fixed 330 fs intervals; (*c*) phase kicks at stochastic intervals averaging 330 fs. The solid lines in (*c*) depict the case of randomized phase kicks whereas the dotted lines indicate π phase kicks. For all simulations, the parameters are $m = 0.00072569 \cdot m_e$, $\alpha = 0.00072569\ hartree \cdot {a_0}^{-1}$, and $\beta = 0.092292\ {a_0}^{-2}$. (The colour version of this figure is included in the online version of the journal.)

to precisely assemble molecules on the solid surface, provided by scanning probe techniques, together with the rich variety of properties characteristic of the molecular systems can make of the sensitized semiconductors a promising alternative for the construction of quantum information devices.

More generally, the effect of stochastic phase kicks in a double-well potential illustrates these striking results in a simple and familiar example. In the low temperature limit, the similarity of the tunnelling in the double-well system foreshadows the similar localization possible with a regular series of phase kicks to the hole wave-packet in the surface complex model. The robustness of the implementation to using random-area pulses, however, becomes important in a realistic system, since the time-dependent environment of the surface complex at finite temperature would make precise tuning of the optical transitions difficult.

Acknowledgments

V.S.B. acknowledges a generous allocation of supercomputer time from the National Energy Research Scientific Computing (NERSC) centre and financial support from Research Corporation, Research Innovation Award # RI0702, a Petroleum Research Fund Award from the American Chemical Society PRF # 37789-G6, a junior faculty award from the F. Warren Hellman Family, the National Science Foundation (NSF) Career Program Award CHE # 0345984, the NSF Nanoscale Exploratory Research (NER) Award ECS # 0404191, the Alfred P. Sloan Fellowship (2005–2006), a Camille Dreyfus Teacher-Scholar Award for 2005, and a Yale Junior Faculty Fellowship in the Natural Sciences (2005–2006). L.G.C. Rego acknowledges the financial support from CNPq/Brazil.

References

[1] W. Potz, Phys. Rev. Lett. **79** 3262 (1997).
[2] E. Frishman, M. Shapiro and P. Brumer, J. Chem. Phys. **110** 9 (1999).
[3] W. Potz, Int. J. Quant. Chem. **85** 398 (2001).
[4] A. Vardi and M. Shapiro, Comments Mod. Phys. **2** D233 (2001).
[5] B.I. Ivlev, Phys. Rev. A **62** Art. No. 062102 (2000).
[6] I. Grigorenko, O. Speer and M.E. Garcia, Phys. Rev. B **65** Art. No. 235309 (2002).
[7] J.M. Villas-Boas, A.O. Govorov and S.E. Ulloa, Phys. Rev. B **69** Art. No. 125342 (2004).
[8] C. Weiss and T. Jinasundera, Phys. Rev. A **72** Art. No. 053626 (2005).
[9] A. Matos-Abiague and J. Berakdar, Phys. Rev. B **69** Art. No. 155304 (2004).
[10] D.H. Dunlap and V.M. Kenkre, Phys. Rev. B **34** 3625 (1986).
[11] F. Grossmann, T. Dittrich, P. Jung, *et al*., Phys. Rev. Lett. **67** 516 (1991).
[12] M. Holthaus, Phys. Rev. Lett. **69** 351 (1992).
[13] J. Zak, Phys. Rev. Lett. **71** 2623 (1993).
[14] Xian-Geng Zhao, J. Phys.: Condens. Matter **6** 2751 (1994).
[15] S.Ya. Kilin, P.R. Berman and T.M. Maevskaya, Phys. Rev. Lett. **76** 3297 (1996).
[16] M. Grifoni, P. Hänngi, Phys. Rep. **304** 229 (1998).
[17] D. Loss and D.P. DiVincenzo, Phys. Rev. A **57** 120 (1998).
[18] S. Lloyd, Science **261** 1589 (1993).
[19] D.P. DiVincenzo, Science **269** 255 (1995).

[20] L.G.C. Rego, S.G. Abuabara and V.S. Batista, Quantum Information & Computation **5** 318 (2005).
[21] L.G.C. Rego, S.G. Abuabara and V.S. Batista, J. Chem. Phys. **122** Art No. 154709 (2005).
[22] L.G.C. Rego and V.S. Batista, J. Am. Chem. Soc. **125** 7989 (2003); S.G. Abuabara, L.G.C. Rego and V.S. Batista, J. Am. Chem. Soc. **127** 18234 (2005).
[23] J. Schnadt, P.A. Brühwiler, L. Ratthey, *et al*., Nature **418** 620 (2002).
[24] R. Huber, J.-E. Moser, M. Grätzel, *et al*., J. Phys. Chem. B **106** 6494 (2002).
[25] J.B. Asbury, E. Hao, Y.Q. Wang, *et al*., J. Phys. Chem. B **105** 4545 (2001).
[26] C.R. Rice, M.D. Ward, M.K. Nazeeruddin, *et al*., New J. Chem.**24** 651 (2000).
[27] W.M. Itano, D.J. Heinzen, J.J. Bollinger, *et al*., Phys. Rev. A **41**, 2295 (1990).
[28] M. Maioli and A. Sacchetti, J. Stat. Phys. **119** 516 (2005).
[29] W. Mönch, Springer Series in Surface Sciences, in *Semiconductor Surfaces and Interfaces*, edited by G. Ertl, H. Lüth and D.L. Mills (Springer, Berlin, 1993).
[30] http://cms.mpi.univie.ac.at/vasp/
[31] G. Kresse, Phys. Rev. B **54** 11169 (1996).
[32] G. Kresse and J. Furthmuller, Comp. Mat. Sci. **6** 15 (1996).
[33] U. Diebold, Surf. Sci. Rep. **48** 53 (2003).
[34] W.H. Zurek, Phys. Rev. D **24** 1516 (1981).
[35] W.H. Zurek, Phys. Rev. D **26** 1862 (1982).
[36] E. Joos and H.D. Zeh, Z. Phys. B **59** 223 (1985).
[37] E. Joos, H.D. Zeh, C. Kiefer, *et al*., *Decoherence and the Appearance of a Classical World in Quantum Theory* (Springer-Verlag, Berlin-Heidelberg, 1996).
[38] E.R. Bittner and P.J. Rossky, J. Chem. Phys. **103** 8130 (1995).
[39] O.V. Prezhdo and P.J. Rossky, Phys. Rev. Lett. **81** 5294 (1998).
[40] K. Shiokawa and R. Kapral, J. Chem. Phys. **117** 7852 (2002).
[41] S.P. McGlynn, L.G. Vanquickenborne, M. Kinoshita, *et al*., *Introduction to Applied Quantum Chemistry* (Holt, Rinehart and Winston Inc., New York, 1972).
[42] J. Cerdá and F. Soria, Phys. Rev. B **61** 7965 (2000).
[43] G.A. Landrum and W.V. Glassy, The YAeHMOP project, http://yaehmop.sourceforge.net
[44] R. Hoffmann, Rev. Mod. Phys. **60** 601 (1988); J.H. Ammeter, H.B. Buergi, J.C. Thibeault, *et al*., J. Am. Chem. Soc. **100**, 3686 (1978).
[45] S.A. Haque, Y. Tachibana, D.R. Klug, *et al*., J. Phys. Chem. B **102** 1745 (1998).
[46] G.S. Agarwal, M.O. Scully and H. Walther, Phys. Rev. Lett. **86** 4271 (2001).
[47] G.S. Agarwal, M.O. Scully and H. Walther, Phys. Rev. A **63** Art. No. 044101 (2001).
[48] L. Viola and S. Lloyd, Phys. Rev. A **58** 2733 (1998).
[49] L. Viola, E. Knill and S. Lloyd, Phys. Rev. Lett. **82** 2417 (1999); **83** 4888 (1999); **85** 3520 (2000).
[50] R. Bavli and H. Metiu, Phys. Rev. Lett. **69** 1986 (1992).
[51] S.G. Abuabara, L.G.C. Rego and V.S. Batista (to be submitted).